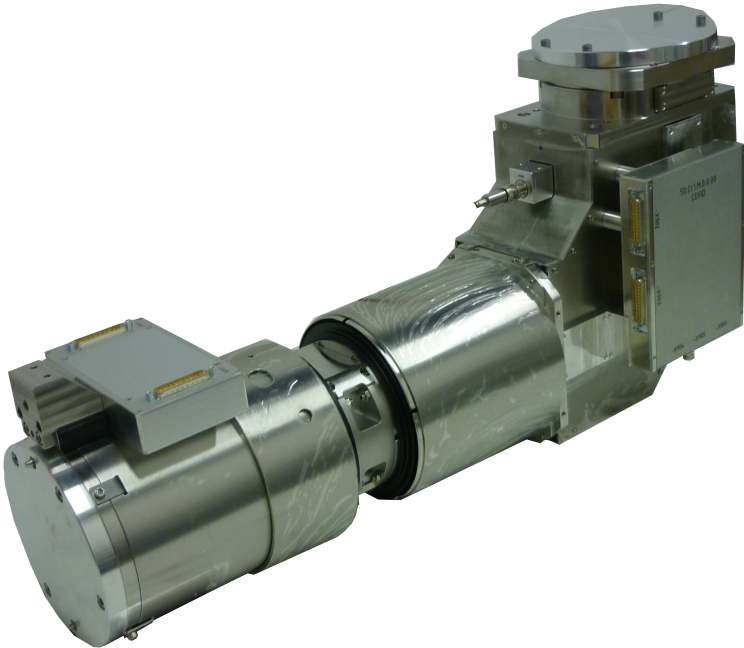


CEFID - CEOS Energy Filtering and Imaging Device

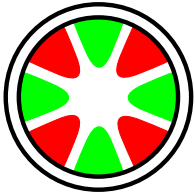
White Paper

Rev. 1.2



CEOS

Corrected Electron Optical
Systems GmbH



CEFID - CEOS Energy Filtering and Imaging Device

Dr. Heiko Müller, Dr. Martin Linck, Dr. Nicole Frindt

CEOS GmbH, Englerstr. 28, 69126 Heidelberg, Germany

info@ceos-gmbh.de

www.ceos-gmbh.de

Tel.: +49 6221 89467-0

Fax: +49 6221 89467-29

1 Application

Energy-Filtered Transmission Electron Microscopy (EFTEM) applications, including Electron Spectroscopic Imaging (ESI) and Electron Energy-Loss Spectroscopy (EELS), for materials science and life science. Especially appropriate for zero-loss filtering and core-loss spectroscopy with high standards in non-isochromaticity, energy resolution and field of view.

2 Introduction

Since the invention of electron energy loss spectroscopy for transmission electron microscopy (TEM) many decades ago this technique has been improved continuously. Today energy filters belong to the standard equipment for high-end TEMs. Post-column energy filters are widely used. These filter solutions allow for a predefined microscope – energy filter – detector combination. However, due to the latest developments in detector technology and in acquisition schemes in Energy-Filtered Transmission Electron Microscopy (EFTEM) the demand for modular components with flexibly configurable interfaces for hardware as well as for software solutions is rapidly increasing. For Electron Spectroscopic Imaging (ESI) as well as for Electron Energy-

Loss-Spectroscopy (EELS) high optical stability and imaging quality of the energy filters are very important, as they form an essential part of the imaging chain.

The new CEFID – CEOS Energy Filtering and Imaging Device meets these customer demands by its remarkably low non-isochromaticity (NI), as well as by its long-term stability and reliable reproducibility of optical alignments after switching between different modes of operation. The combination of low NI with a huge field of view and high stability makes the CEFID very attractive for zero-loss filtering (ESI applications) in life science, especially in combination with a large 4k × 4k detector. In spectroscopy mode (EELS applications) the small NI guarantees an excellent energy resolution. This enables the use of large entrance apertures with better collection efficiency for core-loss spectroscopy. The CEFID platform provides extendable interfaces for detector systems, control and scripting software, advanced user alignments, and data formats, making this post-column filter very flexible and extendable even for customized experimental setups.

A detailed description of the CEFID and its properties can also be found in our paper Kahl et al. [1].

3 Setup and operating mode

Image 1 shows a) a picture and b) a schematic overview of the CEFID Energy Filter. In the following the components of the CEFID are marked by numbers. The energy filter is mounted with a rotatable flange (1) to the bottom of the pre-filter camera housing. A pneumatic aperture (2) is placed at the entrance of the energy filter. The entrance aperture is followed by the pre-slit optics (3), which consist of a sector magnet (4) and several multipole elements (5). Behind the sector element there is the energy selection slit (6) and a quadrupole projective (7) called post-slit optics. At the very end of the energy filter a drift tube (8) and the electron detector (9) are mounted.

The filter entrance aperture can be selected by a pneumatic actuator. Depending on the operating mode the user can choose between four different aperture sizes or other shapes (ESI: 12.5 mm aperture, EELS: 5 mm and 2 mm aperture, filter alignment: quadratic array of 11 x 11 holes).

In the following the essential optical components of the CEFID are explained:

Sector magnet: The pre-slit optics is arranged around a strong sector magnet. It deflects the incoming electron trajectories by 90°. Similar to an optical prism the sector magnet acts as a dispersive element. The electrons are spatially separated by their energy. This enables the visualization of the electron energy-loss spectrum at the energy-selection plane.

The **energy selection slit** is located at the energy-selection plane. Electrons in a defined energy range can be selected for imaging (ESI) whereas other electrons are blocked. The slit mechanics consists of two slit blades which can be moved by piezo driven manipulators with sub- μm positioning accuracy. The dispersion at the slit plane can be adjusted to $3.6 \mu\text{m}/\text{eV}$ at 300 kV. This reproducibly allows for a minimum energy selection window well below 1.0 eV.

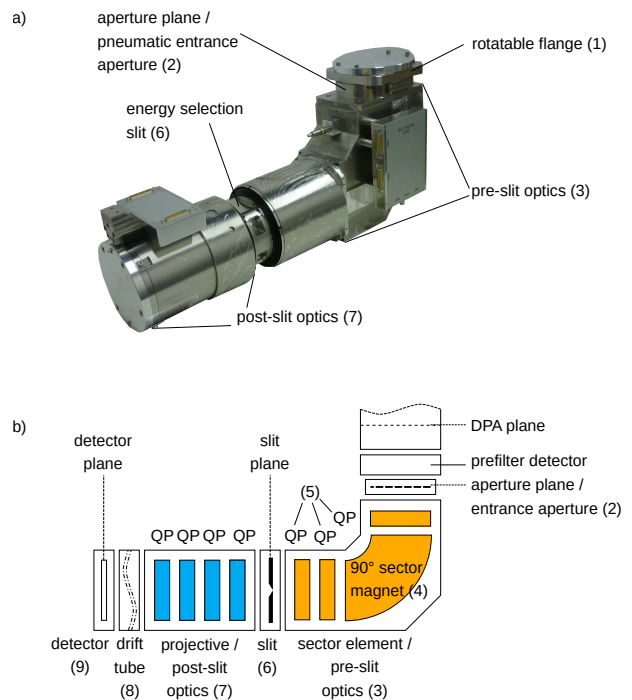


Figure 1: a) Picture and b) schematic overview of the CEFID - CEOS Energy Filtering and Imaging Device.

Multipole elements: Close to the sector magnet there are three multipole lenses. They are marked as „QP“ in figure 1. The first two multipole lenses in front of and behind the sector magnet act as focusing elements. They focus all electrons passing through the entrance aperture into the energy-selection plane. In this process lower and higher order aberrations have to be compensated as good as possible to enable a sharp energy resolution for large entrance apertures. The third multipole lens in front of the energy-selection plane is used to adjust the dispersion introduced by the sector magnet and to correct for the inclination of the spectrum in EELS mode.

Quadrupole objective: The aberration corrected quadrupole objective consists of four quadrupole lenses. It is used to image the energy spectrum from the energy-selection plane onto the detector plane with a huge variable magnification range or to image the object image or rather the diffraction image from the entrance aperture plane onto the detector

plane. For energy-filtered imaging or diffraction the slit at the energy-selection plane is used to select a defined energy window.

The sector magnet and the quadrupole optics are optimized for low aberrations. The unavoidable residual aberrations can be compensated with two 12-pole elements which minimize the residual non-isochromaticity and with six weak stigmators which correct for twofold and threefold aberrations of the quadrupole optics.

Based on this approach a separation of isochromaticity and geometrical distortion can be realized to the greatest possible extent. During the change between spectroscopy (EELS) with different dispersion levels and energy-filtered imaging (ESI) the optical alignment before the energy selection plane remains almost unchanged. This minimizes the alignment time and efforts and simplifies the application workflow.

By default the CEFID is delivered with a 4k x 4k CMOS camera (TVIPS XF416, 15.5 μm pixel size, 48 fps). Other detectors can be installed on request, in an additional camera housing with a customized drift tube length or as supplementary detectors behind a retractable TVIPS XF416R camera at the very end of the filter.

4 Optical Performance

4.1 Experimental setup

To demonstrate the performance of the new CEFID experiments have been performed in two different TEMs. For the ESI applications a JEM-2100F from JEOL with Schottky-FEG at 200 kV was used. The EELS applications were done with an Hitachi HF3300S at 300 kV, with cold-FEG.

4.2 Correction of non-isochromaticity

Two non-isochromaticity (NI) measurements at 200 kV are shown here to demonstrate the NI charac-

teristic of the CEFID. Figure 2 a) shows a NI measurement with a $\varnothing 12$ mm entrance aperture. Figure 2 b) shows the measurement with higher post-magnification for the inner $\varnothing 8$ mm area. Both diagrams use the same scale range for a better comparability. For the $\varnothing 8$ mm measurement the variation of the NI values of course is smaller as for the $\varnothing 12$ mm measurement. However the peak to peak NI values even for the $\varnothing 12$ mm measurement are below 1 eV at 200 kV.

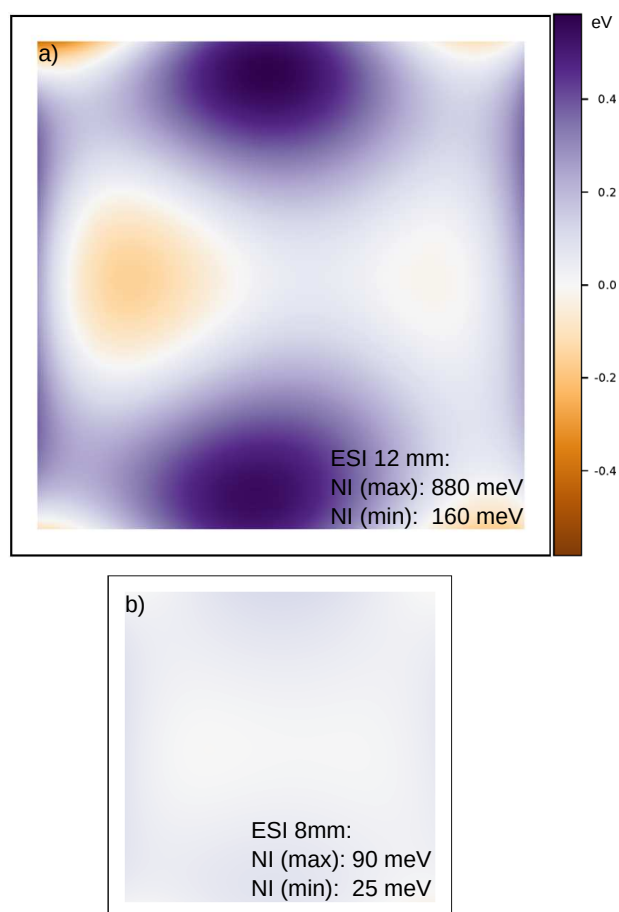


Figure 2: a) Non-isochromaticity measured at 200 kV for the full $\varnothing 12$ mm entrance aperture and b) after increasing the post-magnification and slight retuning for the inner $\varnothing 8$ mm area.

4.3 High quality EEL Spectra

The energy resolution for EELS mode directly depends on the FWHM of the Zero-loss peak (ZLP). Therefore it is essential to minimize the ZLP width at all positions of the EEL spectrum. Figure 3 first row for each energy range shows seven ZLP images at 300 kV for a series of seven equidistant high tension offsets. The high quality of the EEL spectra is demonstrated by the constant shape and width of the ZLPs for different dispersion and spectral ranges from 16 eV to 4096 eV. In addition these excellent spectral properties are demonstrated with a Boron-Nitride sample. Figure 3 second and third row for each energy range show the high quality of the Boron-Nitride spectra together with their line profiles at 300 kV for energy ranges from 16 eV up to 4096 eV.

4.4 Variable spectrum height and data acquisition speed

The spectra of the Boron-Nitride sample were imaged at different spectrum heights. Figure 4 shows three spectra of this sample at identical dispersion corresponding to an energy range of 256 eV for spectrum heights from 2.5% of the total detector height up to 90% detector height. Due to the reduction of the spectrum height the acquisition speed for EELS with a modern CMOS detector like the TVIPS XF416 is drastically increased. This is because these detectors can read out vertical stripe segments of the detector area much faster compared to the whole detector area. This mode of application is of special interest for the field of STEM Spectrum Imaging (SI).

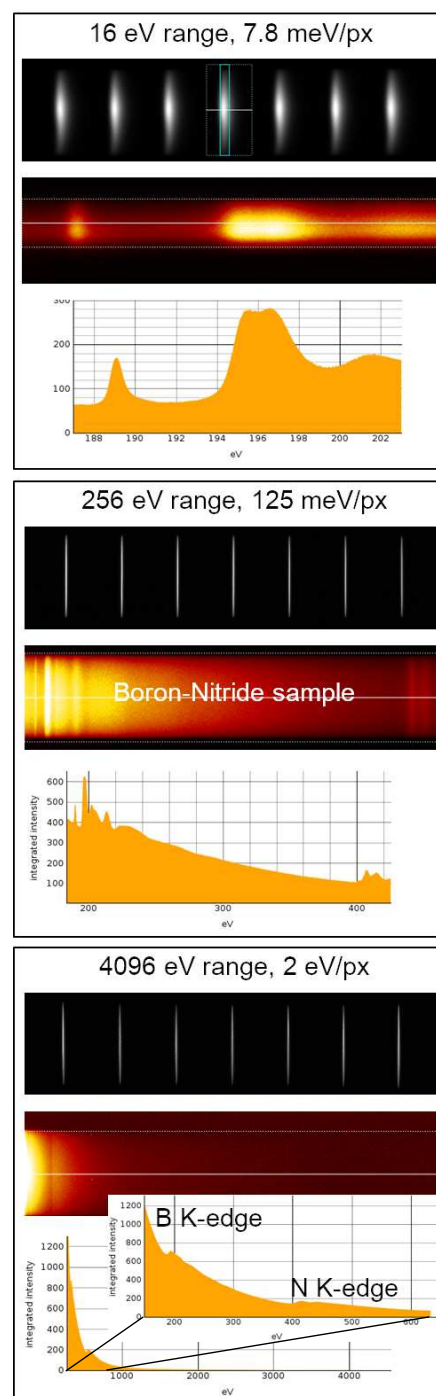


Figure 3: First row: Images of the zero-loss peak at 300 kV for a series of high-tension offsets to illustrate the quality of EEL spectra, the uniform ZLP shape, and distortions-free spectra for different dispersions with energy ranges from 16 eV to 4096 eV. Second and third row: EEL spectra and line scans at 300 kV of Boron-Nitride for energy ranges from 16 eV to 4096 eV.

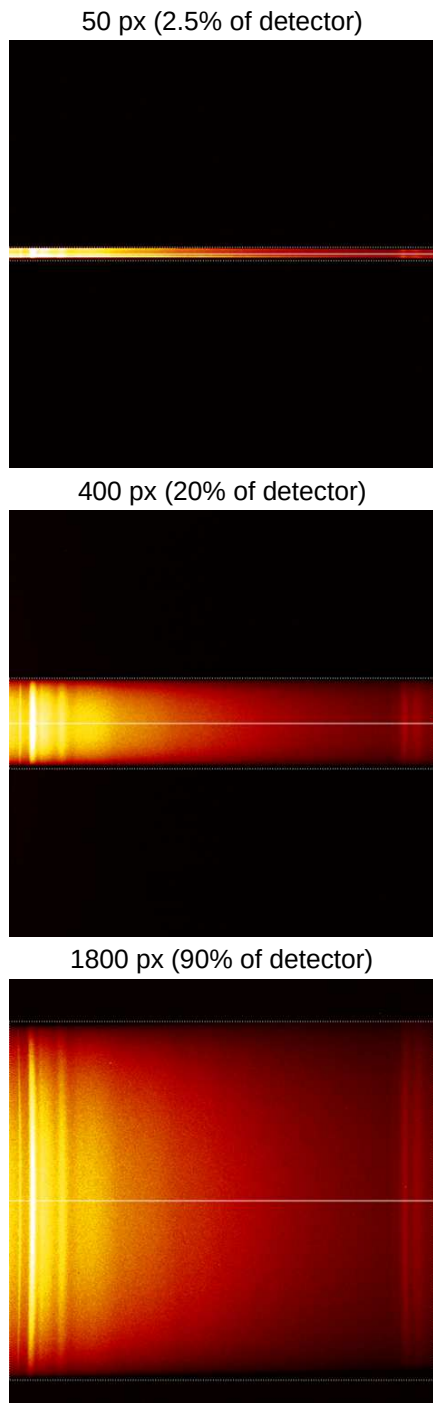


Figure 4: EEL spectrum series of Boron-Nitride at identical dispersion demonstrating flexible spectrum height from 2.5% of detector up to 90% of detector. The measurement was done at 300 kV with cold-FEG and an energy range of 256 eV.

4.5 Long-term stability and accurately reproducible alignment

Many experiments require the ZLP to remain stable in position and focus for a long time. Figure 5 shows experimental data of a ZLP that has been tracked for a period of ~12h. Evidently, the ZLP position changes less than 1eV over such a long time. The remaining small periodical fluctuations can be attributed to the room's air condition cycle and only affect the position on the meV-level. Moreover, the ZLP focus is preserved over the whole measurement time, limited only by the intrinsic energy spread of the cold field emission gun.

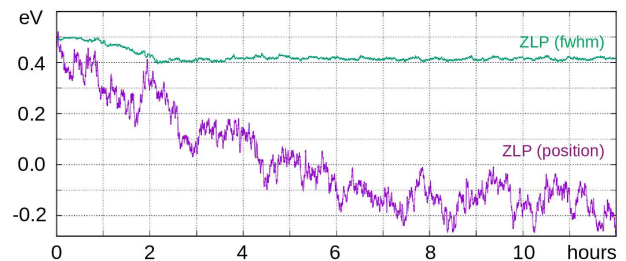


Figure 5: Width and position of ZLP tracked for 12 hours after flashing for a Hitachi HF-3300 300kV Cold-FEG TEM. During the first 2 hours even the decreasing influence of the Boersch effect on the energy width can be observed. The ZLP has a stable position on the sub-eV-Level and moreover remains focused over a long time.

The change of filter operation from EELS to ESI mode and vice versa can be done very easily and shows a very high reproducibility. Figure 6 shows a sequence of images with EEL spectra and an ESI image of a (110)-Silicon sample 200 kV. The ZLP position and the ZLP focus "survive" the related setting changes, hence no re-tuning in between is required at all. This is extremely beneficial to EELS and EFTEM experiments because it allows a continuation in the workflow without interruption for filter-retuning and the operation can focus on the sample features instead.

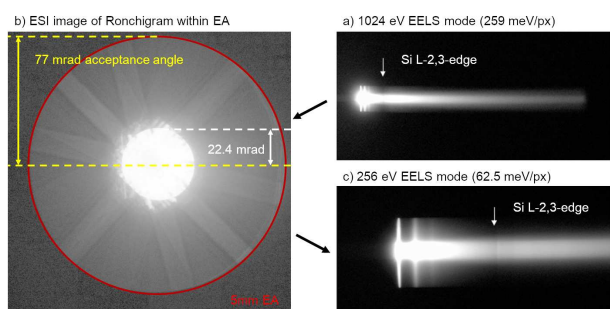


Figure 6: EELS and ESI images of (110)-Silicon sample at 200 kV with Schottky-FEG and entrance aperture (EA) of 5 mm. Switching back and forth between EELS and ESI mode can be done with high accuracy and without retuning.

5 Contributors

We thank our colleagues at CEOS for their support and contributions to the complete development and production process. We are also very grateful to the scientific community and our cooperation partners who stimulated and supported our work on the first CEOS-designed energy filter over many years.

6 References

References

- [1] Frank Kahl, Volker Gerheim, Martin Linck, Heiko Müller, Richard Schillinger, and Stephan Uhlemann. Test and characterization of a new post-column imaging energy filter. *Advances in Imaging and Electron Physics Including Proceedings CPO-10*, page 35, 2019.